Superplastic Behavior and Cavitation in High-Strain-Rate Superplastic Si_3N_{4p}/Al-Mg-Si Composites

HAJIME IWASAKI, TAKASUKE MORI, MAMORU MABUCHI, and KENJI HIGASHI

High-strain-rate superplastic behavior has been investigated for Si_3N_{4p}/Al-Mg-Si (6061) composites with a V_f = 20 and 30 pct, respectively, where V_f is the volume fraction of reinforcements. A maximum elongation was attained at a temperature close to the onset temperature for melting for both composites. The maximum elongation for the 30 vol pct composite was larger than that for the 20 vol pct composite. Development of cavities transverse to the tensile direction is responsible for the lower maximum elongation of the 20 vol pct composite. However, development of the transverse cavities was limited to the optimum superplastic temperature for the 30 vol pct composite. The differential scanning calorimetry (DSC) investigation showed that a sharp endothermic peak appeared for the 30 vol pct composite, indicating that sufficient partial melting occurs. It is, therefore, likely that the stress concentrations are sufficiently relaxed by a liquid phase and that the development of transverse cavities is limited for the 30 vol pct composite.

I. INTRODUCTION

IT has been demonstrated[1–9] that aluminum matrix composites with discontinuous reinforcement materials exhibit high-strain-rate superplasticity. High-strain-rate superplasticity is very attractive for commercial applications, because one of the major problems in the current superplastic forming technique is very slow forming rates of typically 10^{-5} to 10^{-3} s^{-1}.

The mechanisms of high-strain-rate superplasticity for the composites are under debate. The *in situ* transmission electron micrograph (TEM) observation[10] revealed that partial melting occurs at the matrix/reinforcement interfaces and at grain boundaries at elevated temperatures. In addition, experimental results[6,11,12] showed that a maximum elongation is attained at a temperature close to the onset temperature for melting. This suggests that a liquid phase plays an important role in high-strain-rate superplasticity for the composites. It was shown in the previous articles[13,14] that cavities are formed during superplastic deformation for the high-strain-rate superplastic composites as well as for superplastic metals; however, the rate of increase in the cavity volume fraction for the composites is much lower than that for the superplastic 7475 Al alloy. Recently, Wada *et al.*[15] showed that cavity formation is limited by the presence of a liquid phase, because a liquid phase serves to relax the stress concentrations at the matrix/reinforcement interfaces.[16]

In general, a high volume fraction of reinforcements has a deleterious influence on elongations for the composites, because cavity or crack formation is enhanced due to the stress concentrations around the reinforcements. However, if the stress concentrations are sufficiently relaxed by a liquid phase, a high volume fraction of reinforcements may have no deleterious influence on elongation. In the present article, superplastic behavior and cavitation are investigated for two high-strain-rate superplastic Si_3N_{4p}/Al-Mg-Si (6061) composites with a V_f = 20 and 30 pct, respectively, where V_f is the volume fraction of reinforcements. The results in the present investigation showed that, in a superplastic region, a maximum elongation for the 30 vol pct Si_3N_{4p}/Al-Mg-Si composite is larger than that for the 20 vol pct Si_3N_{4p}/Al-Mg-Si composite. This is investigated from the viewpoint of cavitation.

II. EXPERIMENTAL

A fine-grained 20 vol pct Si_3N_{4p}/Al-Mg-Si (6061) composite and a 30 vol pct Si_3N_{4p}/Al-Mg-Si (6061) composite were processed by hot extrusion. The diameter of the Si_3N_4 particulates is less than 1 μm. The details of the fabrication process are given elsewhere.[17] Hot extrusion was carried out at 773 K with a reduction ratio of 100:1. In the previous work,[6] the fine-grained 20 vol pct Si_3N_{4p}/Al-Mg-Si was processed through a similar fabrication procedure; however, the composites used in the present investigation are not the same as the ones in the previous work. Microstructures of the composites are shown in Figure 1. The Si_3N_4 particulates were distributed with reasonable uniformly. No cracks and no cavities were observed prior to straining. The grain size was 2.5 μm for the 20 vol pct composite and 2.1 μm for the 30 vol pct composite, respectively. The differential scanning calorimetry (DSC) experiment[6] was carried out on the as-extruded composites to examine the onset temperature for melting. The heating rate was 10 K/min.

Tensile specimens with a gage length of 5 mm and a gage diameter of 2.5 mm were machined from the as-extruded bars. Constant true-stress tests were carried out at 823 to 853 K for the 20 vol pct composite and at 798 to 833 K for the 30 vol pct composite to investigate superplastic behavior. Each testing temperature range includes temperatures below and above the onset temperature for melting. In addition, constant strain-rate tests were carried

HAJIME IWASAKI, Associate Professor, and TAKASUKE MORI, Professor, are with the Department of Materials Science and Engineering, College of Engineering, Himeji Institute of Technology, Hyogo 671-2201, Japan. MAMORU MABUCHI, Researcher, is with the National Industrial Research Institute of Nagoya, Nagoya 462-0057, Japan. KENJI HIGASHI, Professor, is with the Department of Metallurgy and Materials Science, College of Engineering, Osaka Prefecture University, Osaka 599-8531, Japan.

Manuscript submitted June 27, 1997.

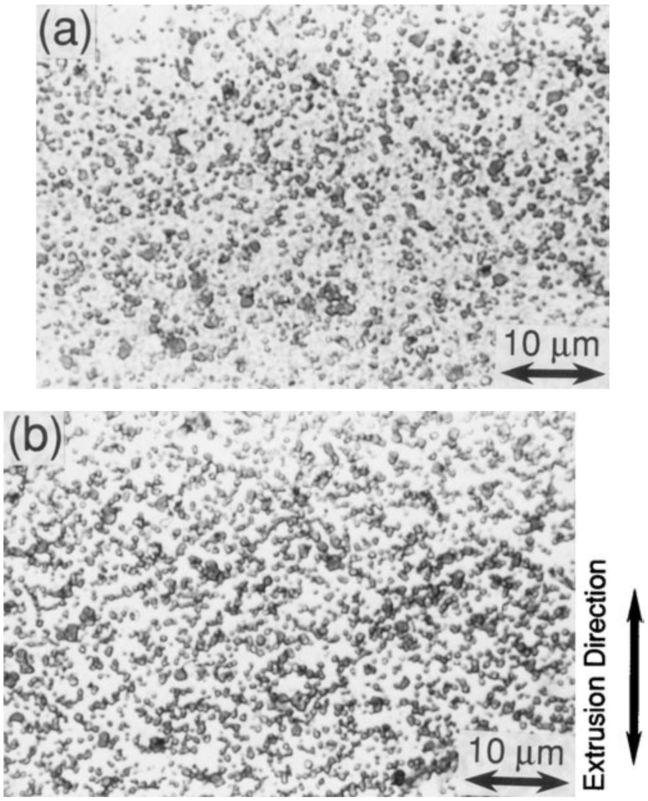

Fig. 1—Microstructures of the as-extruded specimens: (*a*) 20 vol pct Si_3N_{4p}/Al-Mg-Si and (*b*) 30 vol pct Si_3N_{4p}/Al-Mg-Si.

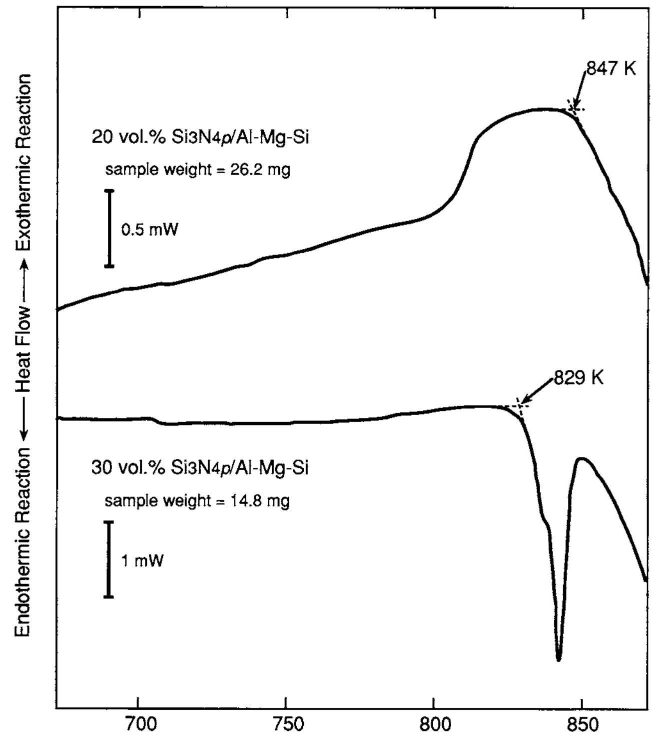

Fig. 2—DSC experimental data from 673 to 873 K.

out at 293 and 713 K to investigate the tensile properties in a solid state with no liquid phase. The tensile axis was selected to be parallel to the extrusion direction. The specimens required about 1.8 ks to equilibrate at the test temperature prior to initiation of straining for all tests.

After the specimens were deformed to predetermined strains, the volume fraction of cavities in the gage length was determined using density measurements (hydrostatic weighing in water with a corresponding gage head used as a density standard). In addition, cavities were metallographically observed using an HITACHI S-900 high-resolution scanning electron microscope (SEM) and the cavity size distributions were analyzed, assuming that all cavities were spherical, using a LUZEX F stereo analyzing system connected to the SEM.

III. RESULTS

A. *DSC Investigation*

The DSC experimental data from 673 to 873 K are shown in Figure 2. For the 20 vol pct composite, an exothermic curve was found and then a continuous endothermic curve appeared. For the 30 vol pct composite, a flat area was found, then a sharp endothermic peak was found, and, finally, a continuous endothermic curve appeared. The onset temperature for melting can be determined from an intercept of the two dotted lines shown in Figure 2. The onset temperature for melting is 847 K for the 20 vol pct composite and 829 K for the 30 vol pct composite, respectively. The partial melting is due to solute segregation.[10,18] The difference in the onset temperature for melting between the 20 vol pct composite and the 30 vol pct composite is probably attributed to the difference in the concentration of segregation.

B. *Superplastic Behavior*

The variation in strain rate (top figure) and elongation to failure (bottom figure), as a function of stress at 823 to 853 K, are shown for the 20 vol pct composite in Figure 3, where the strain rate is determined at $\varepsilon = 0.1$. The strain rate increases with increasing stress at all temperatures. In the equation $\dot{\varepsilon} = A\sigma^n$, $\dot{\varepsilon}$ is the strain rate, A is a constant incorporating structural and temperature dependencies, σ is the stress, and n is the stress exponent that is evaluated by the slope of the curves. The stress exponent values are very high in a low-strain-rate range below 10^{-1} s^{-1}. However, the stress exponent decreases with increasing stress; the low-stress exponent of about 3 is attained at 823 and 833 K, and the low-stress exponent of about 2 is attained at 848 and 853 K. The high-stress exponent in a low-strain-rate range probably results from the presence of a threshold stress.[19]

A maximum elongation of 380 pct is attained at 848 K and at 5 MPa for the 20 vol pct composite, where the strain rate is 5×10^{-1} s^{-1}. It should be noted that the optimum superplastic temperature of 848 K is very close to the onset temperature for melting (847 K).

The variation in strain rate (top figure) and elongation to failure (bottom figure), as a function of stress at 798 to 833 K, are shown for the 30 vol pct composite in Figure 4, where the strain rate is determined at $\varepsilon = 0.1$. For the 30 vol pct composite as well, the stress exponent values are very high in a low-strain-rate range below 10^{-1} s^{-1}. However, the stress exponent decreases with increasing stress; the low-stress exponent of about 3 is attained at 798 and

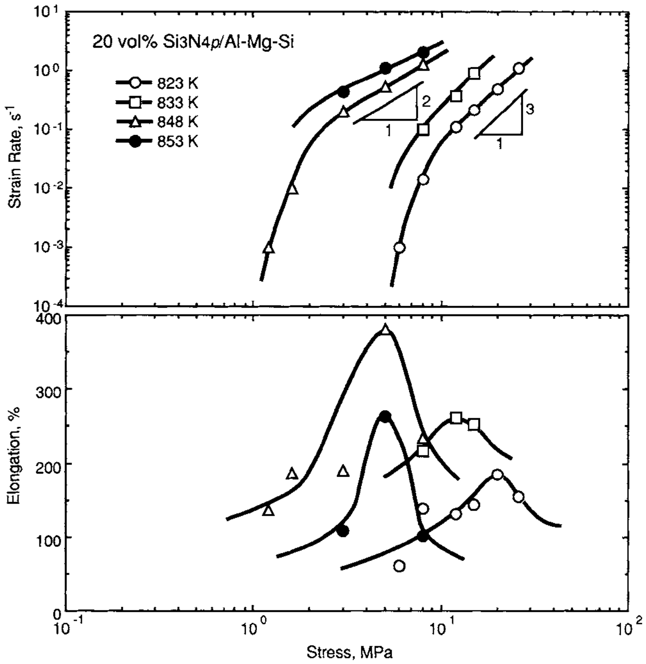

Fig. 3—The variation in strain rate (top figure) and elongation to failure (bottom figure) as a function of stress at 823 to 853 K for the 20 vol pct Si_3N_{4p}/Al-Mg-Si.

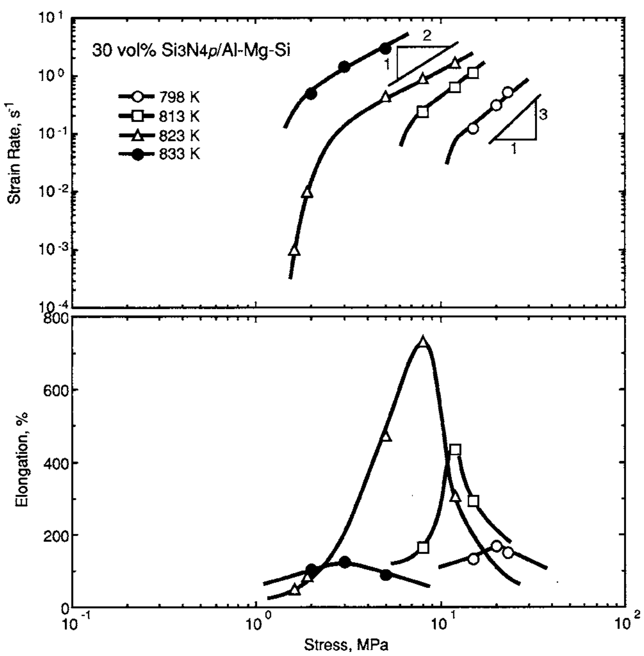

Fig. 4—The variation in strain rate (top figure) and elongation to failure (bottom figure) as a function of stress at 798 to 833 K for the 30 vol pct Si_3N_{4p}/Al-Mg-Si.

813 K, and the low-stress exponent of about 2 is attained at 823 and 833 K.

A maximum elongation of 734 pct is attained at 823 K and at 8 MPa for the 30 vol pct composite, where the strain rate is 9×10^{-1} s^{-1}. The optimum superplastic temperature of 823 K is close to the onset temperature for melting (829 K). It should be noted that the maximum elongation for the 30 vol pct composite is larger than that for the 20 vol pct composite.

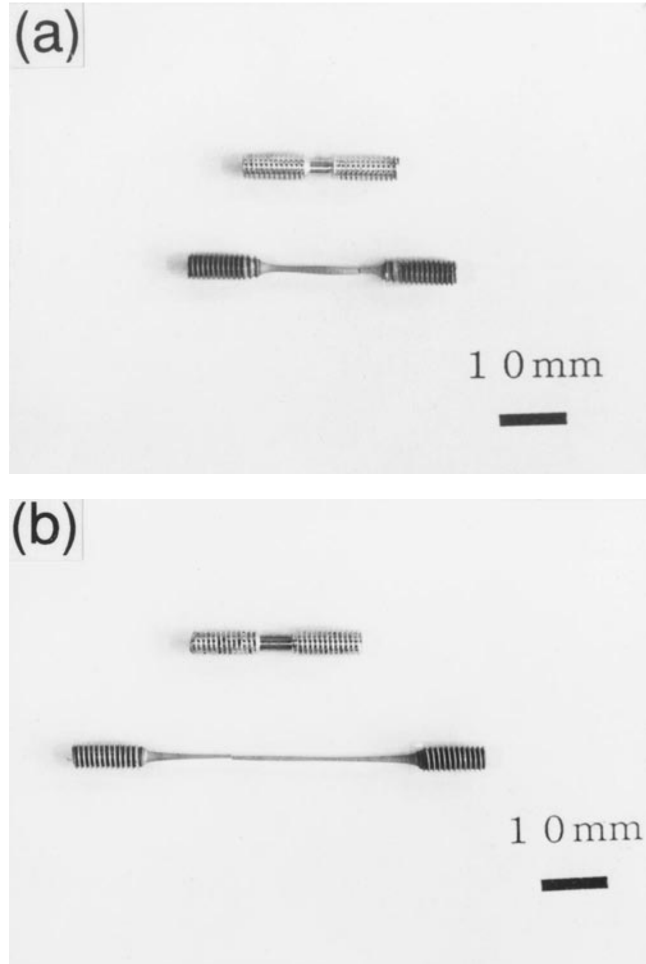

Fig. 5—The specimens deformed at the optimum testing conditions: (*a*) 848 K and 5 MPa for 20 vol pct Si_3N_{4p}/Al-Mg-Si and (*b*) 823 K and 8 MPa for 30 vol pct Si_3N_{4p}/Al-Mg-Si.

The specimens deformed at the optimum testing conditions are shown in Figure 5. Large elongation is attained without development of sharp necking for both specimens. This likely results from the high plastic stability due to the low-stress exponent of about 2. It appears that development of sharp necking is not responsible for the lower maximum elongation of the 20 vol pct composite.

C. *Cavitation*

Cavity nucleation in the specimens deformed at the optimum testing conditions is shown in Figure 6, where the specimens are deformed to $\varepsilon = 0.2$. It can be seen that microcavities are formed at the matrix/reinforcement interfaces. This trend is the same as that presented in the previous articles.[13,14,20]

The variation in volume fraction of cavities as a function of true strain is shown in Figure 7, where the specimens are deformed at the optimum testing conditions. It should be noted that the volume fraction of cavities for the 30 vol pct composite is larger than that for the 20 vol pct composite. Therefore, the lower maximum elongation for the 20 vol pct composite cannot be explained from the viewpoint of the cavity volume fraction.

It is recognized that cavities grow during superplastic

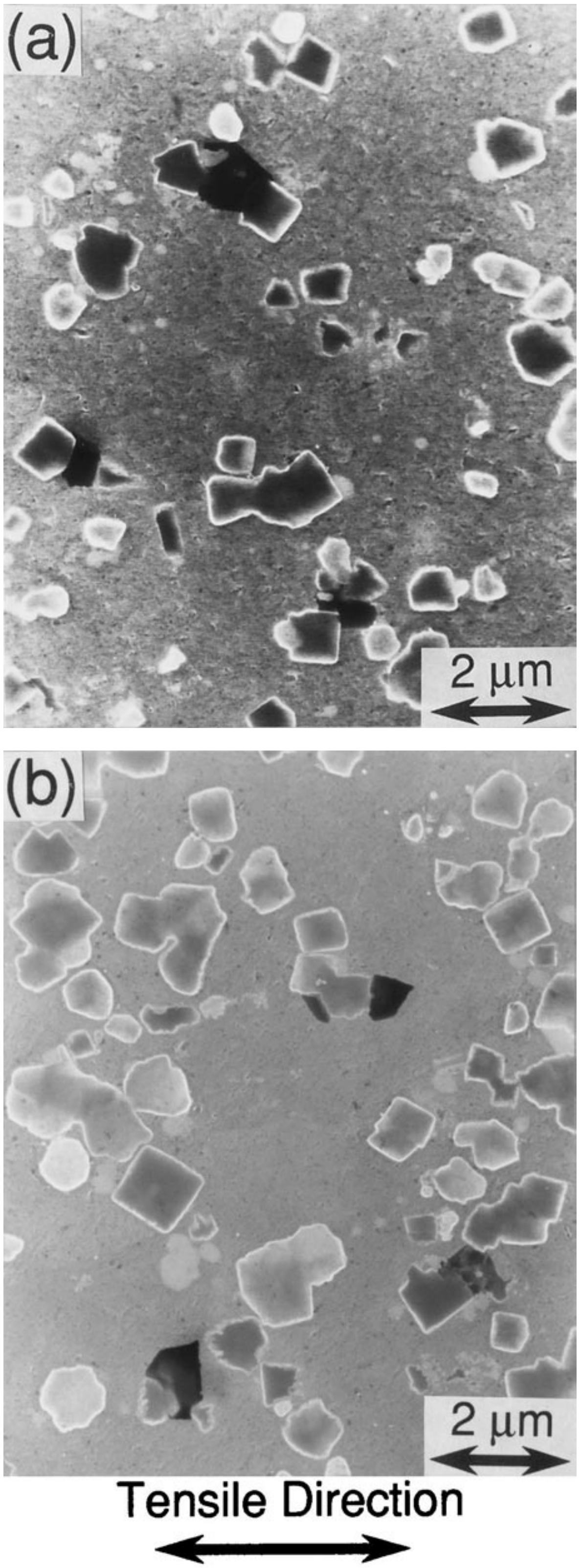

Fig. 6—Cavity nucleation in the specimens deformed to $\varepsilon = 0.2$: (*a*) 848 K and 5 MPa for 20 vol pct Si_3N_{4p}/Al-Mg-Si and (*b*) 823 K and 8 MPa for 30 vol pct Si_3N_{4p}/Al-Mg-Si. The tensile axis is horizontal.

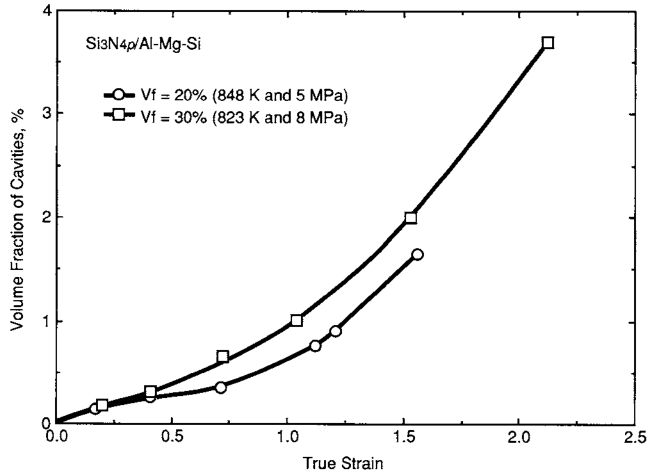

Fig. 7—The variation in volume fraction of cavities as a function of true strain.

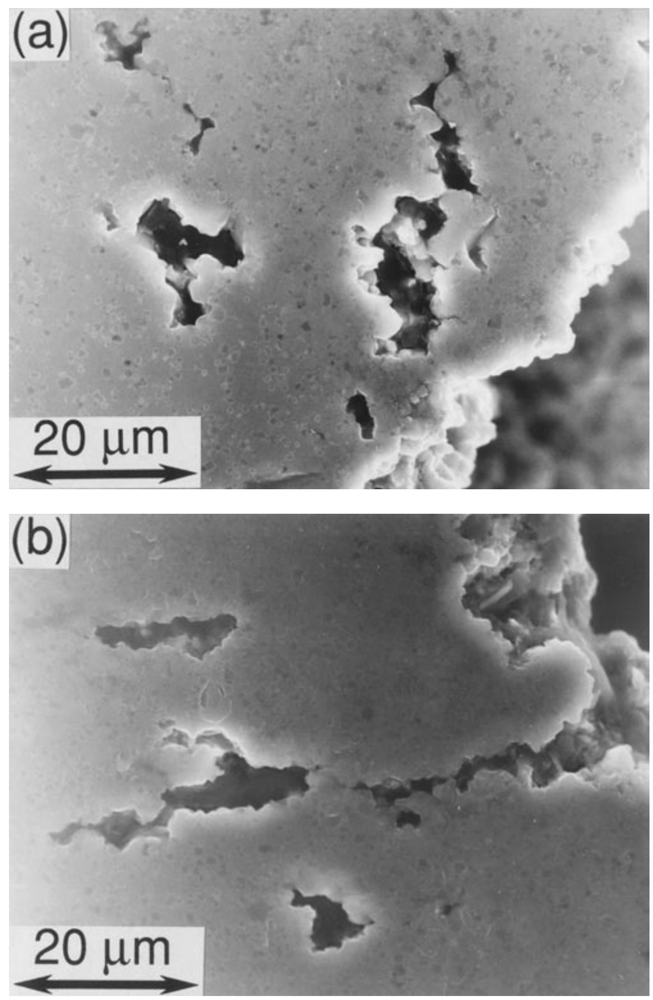

Fig. 8—Microstructures near fracture surface in the specimens deformed at the optimum testing conditions: (*a*) 848 K and 5 MPa for 20 vol pct Si_3N_{4p}/Al-Mg-Si and (*b*) 823 K and 8 MPa for 30 vol pct Si_3N_{4p}/Al-Mg-Si. The tensile axis is horizontal.

deformation and that interlinkage of cavities gives rise to premature fracture.[21,22,23] Microstructures near the fracture surface in the specimens deformed at the optimum testing conditions are shown in Figure 8. It can be seen that for the 30 vol pct composite, cavities are elongated in the tensile direction; however, cavities tend to be developed transverse to the tensile direction for the 20 vol pct composite.

Table I. Summary of the Tensile Properties for the Si_3N_{4p}/Al-Mg-Si

Materials	Temperature, K	Stress, MPa	Strain Rate, s^{-1}	Elongation, Pct	m Value
20 vol pct Si_3N_{4p}/Al-Mg-Si	293*	311†	2×10^{-1}	10	—
	713*	71†	6×10^{-1}	46	0.2
	848**	5	5×10^{-1}‡	380	0.5
30 vol pct Si_3N_{4p}/Al-Mg-Si	293*	423†	2×10^{-1}	6	—
	713*	82†	6×10^{-1}	40	0.2
	823**	8	9×10^{-1}‡	734	0.5

*Constant strain-rate tests.
**Constant stress tests.
†The stress is determined at $\varepsilon = 0.1$.
‡The strain rate is determined at $\varepsilon = 0.1$.

Development of the transverse cavities is likely responsible for the premature fracture of the 20 vol pct composite.

IV. DISCUSSION

The maximum elongation is attained at a temperature close to the onset temperature for melting for both composites. This indicates that a liquid phase plays an important role in high-strain-rate superplasticity for the composites. It is important to investigate the tensile properties and cavitation in a solid state with no liquid phase in order to understand the role of a liquid phase. Because the eutectic temperature in aluminum solid solution is 723 K for the Al-Mg solid phase and 850 K for the Al-Si solid phase, melting never occurs at temperatures less than 723 K. Hence, in the present investigation, additional tensile tests were conducted at 293 and 713 K to investigate the tensile properties and cavitation in a solid state with no liquid phase. Results of the tensile tests are listed in Table I. The strain-rate sensitivity (m) at 713 K was examined by change-in-strain-rate tests. It should be noted that at the optimum superplastic conditions, a maximum elongation for the 30 vol pct composite is larger than that for the 20 vol pct composite; however, the former exhibits smaller elongation at 293 and 713 K than the latter.

The cavity size distribution in the specimens deformed to $\varepsilon = 0.7$ is shown in Figure 9, where cavities are assumed to be spherical. It is noted that cavity formation is more enhanced at the optimum superplastic temperature than at 713 K, independent of the volume fraction of reinforcements. It can be seen that more and larger cavities are formed for the 30 vol pct composite than for the 20 vol pct composite. Therefore, the larger maximum superplastic elongation for the 30 vol pct composite cannot be explained from the analysis of the cavity size distribution.

Typical cavities in the specimens deformed at 713 K are shown in Figure 10. It is noted that cavities are developed transverse to the tensile direction for both composites. In general, a cavity grows by diffusion and by plastic deformation of the matrix around a cavity, and, finally, interlinkage of cavities in the direction transverse to the tensile axis gives rise to fracture. For high-strain-rate superplastic composites, the dominant mechanism of cavity growth is not diffusion, but plastic deformation of the surrounding matrix, since the amount of mass transfer by diffusion is very little due to a too-short time.[24] When cavity growth is controlled by plastic deformation of the surrounding matrix, a cavity tends to be elongated in the tensile directions.

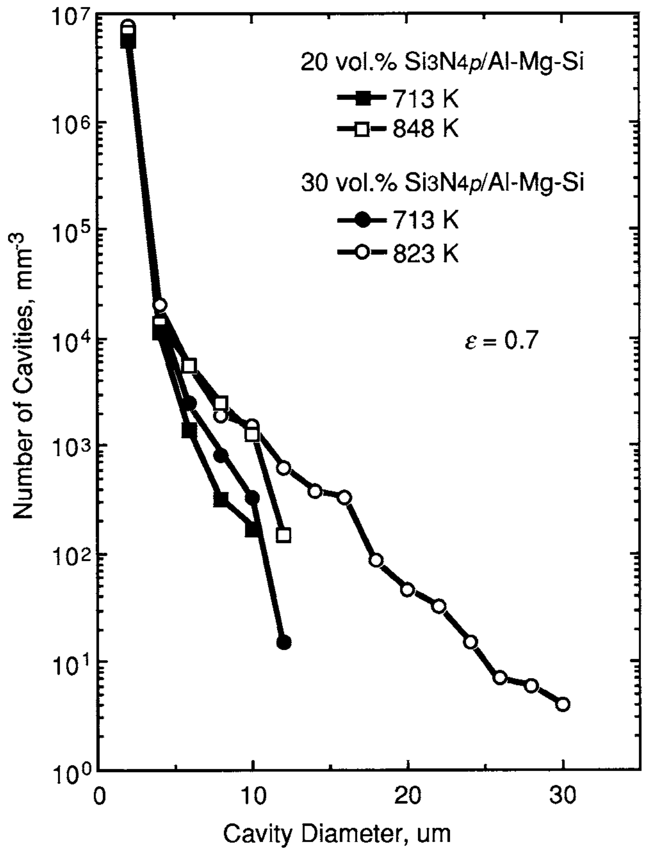

Fig. 9—The cavity size distribution in the specimens deformed to $\varepsilon = 0.7$.

For the 30 vol pct composite, cavities are elongated in the tensile direction in the specimen deformed at the optimum superplastic conditions. However, cavities are developed transverse to the tensile direction in the specimen deformed at the optimum superplastic temperature for the 20 vol pct composite, as shown in Figure 8. Similarly, cavities are developed transverse to the tensile direction in the specimens deformed at 713 K for both composites. In general, stress concentrations are caused around the reinforcements during deformation of the composites. The stress concentrations are probably responsible for the development of the transverse cavities.

The DSC investigations showed that, while a sharp endothermic peak appeared for the 30 vol pct composite, no sharp endothermic peak was found for the 20 vol pct composite. This suggests that sufficient partial melting occurs

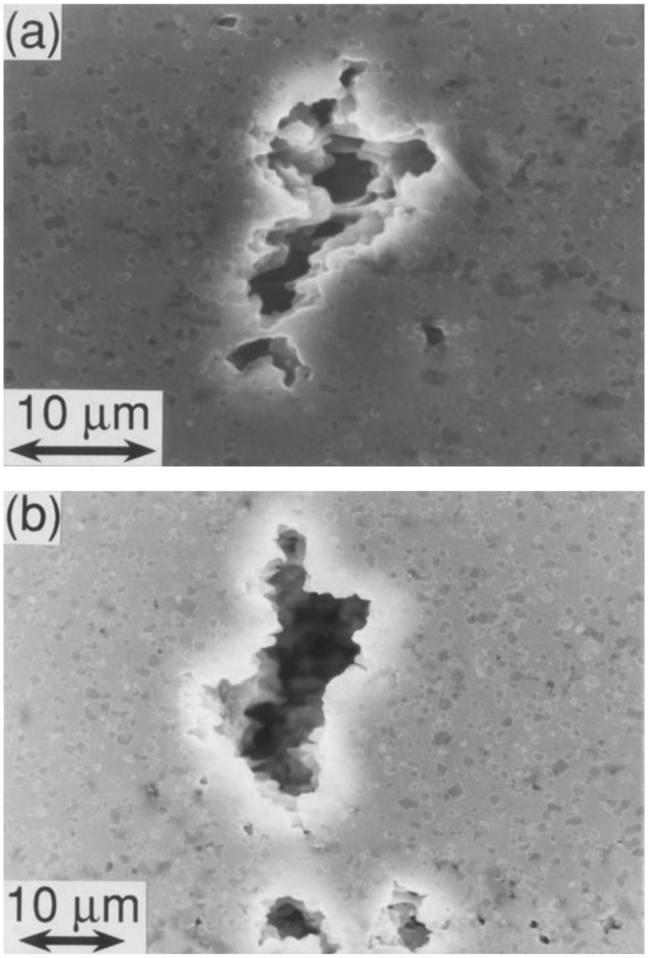

Fig. 10—Typical cavities in the specimens deformed at 713 K: (*a*) 20 vol pct Si_3N_{4p}/Al-Mg-Si and (*b*) 30 vol pct Si_3N_{4p}/Al-Mg-Si. The tensile axis is horizontal.

at the interface and grain boundary sites at the onset temperature for melting of the 30 vol pct composite. Therefore, for the 30 vol pct composite, the stress concentrations can be relaxed by the presence of a liquid phase.[16] However, the fact that no sharp endothermic peak appeared for the 20 vol pct composite suggests that insufficient partial melting occurs, even at the onset temperature, for melting. In this case, the stress concentrations are insufficiently relaxed. Insufficient relaxation of the stress concentrations likely gives rise to premature fracture because of the development of the transverse cavities. Therefore, the fact that, in a superplastic region, the maximum elongation for the 30 vol pct composite was larger than that for the 20 vol pct composite is probably because the stress concentrations are sufficiently relaxed by a liquid phase and the development of transverse cavities is limited for the 30 vol pct composite.

V. CONCLUSIONS

1. High-strain-rate superplastic behavior was investigated for 20 vol pct Si_3N_{4p}/Al-Mg-Si and 30 vol pct Si_3N_{4p}/Al-Mg-Si composites. A maximum elongation was attained at a temperature close to the onset temperature for melting for both composites. This indicates that a liquid phase plays an important role in high-strain-rate superplasticity for the composites.
2. The maximum elongation for the 30 vol pct composite was larger than that for the 20 vol pct composite. The larger maximum elongation for the 30 vol pct composite could not be explained from the viewpoint of plastic stability, cavity volume fracture, and cavity size distribution.
3. Cavities were developed transverse to the tensile direction for the 20 vol pct composite. This is responsible for the premature fracture of the 20 vol pct composite.
4. Development of the transverse cavities was limited for the 30 vol pct composite. In DSC investigation, a sharp endothermic peak appeared for the 30 vol pct Si_3N_{4p}/Al-Mg-Si composite, indicating that sufficient partial melting occurs. It is, therefore, likely that a liquid phase due to sufficient partial melting serves to relax the stress concentrations, and, thereby, development of the transverse cavities is limited for the 30 vol pct composite.

ACKNOWLEDGMENTS

Two of the authors (HI and KH) gratefully acknowledge the financial support of the Ministry of Education, Science and Culture of Japan provided by a grant-in-aid and also KH acknowledges the support from the United States Army Research Office under Grant No. DAAH04-94-G-0070, monitored by Drs W. Simmons and I. Ahmad.

REFERENCES

1. T.G. Nieh, C.A. Henshall, and J. Wadsworth: *Scripta Metall.*, 1984, vol. 18, pp. 1405-08.
2. T. Imai, M. Mabuchi, Y. Tozawa, and M. Yamada: *J. Mater. Sci. Lett.*, 1990, vol. 9, pp. 255-57.
3. H. Xiaoxu, L. Qing, C.K. Yao, and Y. Mei: *J. Mater. Sci. Lett.*, 1991, vol. 10, pp. 964-66.
4. M. Mabuchi, K. Higashi, Y. Okada, S. Tanimura, T. Imai, and K. Kubo: *Scripta Metall. Mater.*, 1991, vol. 25, pp. 2517-22.
5. K. Higashi, T. Okada, T. Mukai, S. Tanimura, T.G. Nieh, and J. Wadsworth: *Scripta Metall. Mater.*, 1992, vol. 26, pp. 185-90.
6. M. Mabuchi and K. Higashi: *Mater. Trans. JIM*, 1994, vol. 35, pp. 399-405.
7. M. Mabuchi, K. Higashi, and T.G. Langdon: *Acta Metall. Mater.*, 1994, vol. 42, pp. 1739-45.
8. K.C. Chan, B.Q. Han, and T.M. Yue: *Acta Mater.*, 1996, vol. 44, pp. 2515-22.
9. B.Q. Han and K.C. Chan: *Scripta Mater.*, 1997, vol. 36, pp. 593-98.
10. J. Koike, M. Mabuchi, and K. Higashi: *Acta Metall. Mater.*, 1995, vol. 43, pp. 199-206.
11. M. Mabuchi and K. Higashi: *Mater. Sci. Eng.*, 1994, vols. A179–A180, pp. 625-27.
12. K. Higashi, T.G. Nieh, M. Mabuchi, and J. Wadsworth: *Scripta Metall. Mater.*, 1995, vol. 32, pp. 1079-84.
13. H. Iwasaki, M. Takeuchi, T. Mori, M. Mabuchi, and K. Higashi: *Scripta Metall. Mater.*, 1994, vol. 31, pp. 255-60.
14. H. Iwasaki, M. Mabuchi, K. Higashi, and T.G. Langdon: *Mater. Sci. Eng.*, 1996, vol. A208, pp. 116-21.
15. S. Wada, M. Mabuchi, K. Higashi, and T.G. Langdon: *J. Mater. Res.*, 1996, vol. 11, pp. 1755-63.
16. M. Mabuchi and K. Higashi: *Phil. Mag. Lett.*, 1994, vol. 70, pp. 1-6.
17. M. Mabuchi, T. Imai, and K. Higashi: *J. Mater. Sci.*, 1993, vol. 28, pp. 6582-86.
18. J. Koike, M. Mabuchi, and K. Higashi: *J. Mater. Res.*, 1995, vol. 10, pp. 133-38.

19. R.S. Mishra, T.R. Bieler, and A.K. Mukherjee: *Acta Metall. Mater.*, 1995, vol. 43, pp. 877-91.
20. H. Iwasaki, M. Mabuchi, and K. Higashi: *Mater. Sci. Technol.*, 1996, vol. 12, pp. 505-12.
21. D.W. Livesey and N. Ridley: *Metall. Trans. A*, 1978, vol. 9A, pp. 519-26.
22. C.C. Bampton and J.W. Edington: *Metall. Trans. A*, 1982, vol. 13A, pp. 1721-27.
23. A.H. Chokshi and T.G. Langdon: *Acta Metall.*, 1990, vol. 38, pp. 867-77.
24. H. Iwasaki, M. Mabuchi, and K. Higashi: *Acta Mater.*, 1997, vol. 45, pp. 2759-2764.